Influence of Pretreatment on Lanthanum Nitrate, Carbonate, and Oxide Powders

B. Klingenberg and M. Albert Vannice*

Department of Chemical Engineering, The Pennsylvania State University, University Park, Pennsylvania 16802-4400

Received May 2, 1996. Revised Manuscript Received July 17, 1996[⊗]

Diffuse reflectance FTIR spectra, X-ray diffraction patterns, and BET surface areas of $La(NO_3)_3$, $La_2(CO_3)_3$, and La_2O_3 have been obtained after various stages of thermal decomposition in the presence and absence of O_2. In situ DRIFTS provided information about the surface chemistry taking place during the adsorption of NO and CO_2 on the La oxide surfaces obtained. Decomposition of $La(NO_3)_3$ under flowing Ar at 773 K resulted in a mixture of La_2O_3 and a nitrate phase with ionic (noncoordinated) nitrate groups, i.e., those not directly coordinated to a La cation. However, when the decomposition was performed under flowing O_2, $LaONO_3$ was the principal compound. NO adsorption on the oxide surface after decomposition enhanced the peak intensity of residual nitrate surface species—no new peaks appeared. $La_2(CO_3)_3$ was more stable and was only partly transformed into $La_2O_2CO_3$ during thermal treatment at 773 K. The commercial La_2O_3 samples contained mainly hydroxide if exposed to, or stored under, ambient air. The $La(OH)_3$ decomposes when heated to 773 K, but rehydroxylation occurs rapidly if the samples are exposed to ambient air. Both the temperature and the gaseous medium of the calcination pretreatment determine the final state of the material. High temperatures (>1173 K) and a CO_2-free medium must be used to guarantee transformation into principally La_2O_3, which still contains variable amounts of surface or subsurface carbonate groups. However, these high calcination temperatures result in considerable loss of surface area. Bidentate and unidentate carbonates were formed on La_2O_3 by adsorbing CO_2 at either 298 or 773 K, thus revealing the surface sites have medium Lewis basicity. NO adsorption at 298 and 773 K leads to an exchange reaction with carbonate ions to disproportionate NO and form nitrate and nitrite groups, N_2 and CO_2. These results provide comprehensive references for the preparation and characterization of catalytic La_2O_3 surfaces.

1. Introduction

Recent studies have revealed that lanthanum oxide shows promise as a catalyst for the reduction of NO by methane in the presence of O_2.[1−4] This catalytic reaction, under lean-burn conditions, has attracted increasing attention as it is important for emission control in industrial processes and lean-burn automotive engines. In an effort to optimize catalytic performance, it is of particular interest to understand the surface chemistry involved in this reaction mechanism and to determine the state of the surface during the catalytic process. Studies of kinetic behavior have already provided a significant body of data on the catalytic performance of La_2O_3 for NO reduction by CH_4,[1−4] and on the basis of these results, possible catalytic sequences have been proposed.[5] It is desirable to test these reaction sequences by identifying any surface species formed by adsorption of the reactants as well as by characterizing the catalyst itself prior to and under reaction conditions. This is of particular interest because it is well-known that the composition and activity of La_2O_3 for other catalytic reactions, such as methane oxidative coupling (MOC), is highly dependent on the preparation and activation procedures used.[6,7] Taylor and Schrader[6] studied different starting materials, such as La_2O_3, $La_2(CO)_3$, $La_2O_2CO_3$, and $LaCO_3OH$, and observed that under reaction conditions (973−1073 K) the formation of the oxide primarily occurred. Nevertheless, different activities for methane conversion and selectivities to ethylene were reported, and the presence of the II-$La_2O_2CO_3$ (hexagonal) phase was assumed to be especially beneficial. A recent study by Lacombe et al.[7] emphasized again the relationship between morphology and catalytic performance of La_2O_3 for MOC and proposed a reaction mechanism for methane oxidation based on structural sensitivity and active sites. Le Van et al.[8,9] showed that the dioxycarbonate was formed during MOC at temperatures between 873 and 923 K as a result of deep methane oxidation on the catalyst surface, and it decomposed at higher temperatures.

* To whom correspondence should be addressed.

[⊗] Abstract published in *Advance ACS Abstracts,* September 1, 1996.

(1) Zhang, X.; Walters, A. B.; Vannice, M. A. *Appl. Catal.* **1994**, *B4*, 237.
(2) Zhang, X.; Walters, A. B.; Vannice, M. A. *J. Catal.* **1995**, *155*, 290.
(3) Zhang, X.; Walters, A. B.; Vannice, M. A. *Catal. Today* **1995**, *27*, 41.
(4) Zhang, X.; Walters, A. B.; Vannice, M. A. *Appl. Catal. B* **1996**, *7*, 321.
(5) Zhang, X.; Walters, A. B.; Vannice, M. A. *J. Catal.* **1996**, *159*, 119.
(6) Taylor, R. P.; Schrader G. L. *Ind. Eng. Chem. Res.* **1991** *30*, 1016.
(7) Lacombe, S.; Geantet, C.; Mirodatos, C. *J. Catal.* **1994**, *151*, 439.
(8) Le Van, T.; Che, M.; Kermarec, M.; Louis, C.; Tatibouët, J. M. *Catal. Lett.* **1990**, *6*, 395.
(9) Le Van, T.; Che, M.; Tatibouët, J. M.; Kermarec M. *J. Catal.* **1993**, *142*, 18.

S0897-4756(96)00255-4 CCC: $12.00

Lanthanum oxide is known to be very sensitive to water and carbon dioxide,[10,11] thus, preparation in or exposure to ambient air leads to bulk hydroxylation as well as carbonation, which is suggested to occur mainly through the formation of surface carbonates or hydroxycarbonates.[10] While the hydroxyl compounds are readily removed by heating to 573 K,[12,13] the carbonate phases are decomposed only by thermal treatment at 973−1073 K, and it is generally accepted that dioxycarbonates are formed as intermediates in the decomposition.[10,14,15] These studies have clearly shown that a variety of compounds may exist in La_2O_3, and their presence depends on the pretreatment utilized.

These previous results impact on the work presented in this paper because they verify that "La_2O_3" catalysts can exhibit large variations in composition and chemistry. The catalytic studies of NO reduction with methane were performed under conditions (773−973 K) comparable to those used by Lacombe et al. and LeVan et al.[7−9] Changes in composition and the formation of mixed nitrate and carbonate phases, especially at the surface, are likely to occur, and it is probable that particular phases are closely associated with catalytic performance, as they determine the type and availability of active sites. Thus, it is important to know the state of the catalyst that exists as a result of pretreatment and activation procedures. Different preparative procedures for La_2O_3 catalysts are described in the literature. In general, starting materials such as La_2O_3 (commercial), $La(OH)_3$, or $La(NO_3)_3$ are calcined at high temperature to remove nitrate, hydroxyl, and carbonate species,[6,8,9,14] and, in particular, decomposition of the nitrate precursor is used when supported catalysts are prepared via aqueous impregnation.[16−19] However, the high temperatures needed for complete decomposition of the carbonate and nitrate groups have a nondesirable side effect for catalytic applications as they result in considerable loss of surface area. Hence, the chosen pretreatment may require a compromise between these two considerations, and it is thus of particular interest to understand the phase composition of the catalysts after a respective treatment. In accordance, this paper presents a thorough study by in situ diffuse reflectance FTIR spectroscopy (DRIFTS) and X-ray diffraction (XRD) of the catalytic La_2O_3 materials, as well as the $La_2(CO_3)_3$ and $La(NO_3)_3$ precursors. The influence of different pretreatments on commercial La_2O_3 samples is examined, and the behavior of lanthanum compounds during thermal treatment is reported. It is advantageous that the use of in situ FTIR can exclude the influence of atmospheric air (hence CO_2 and H_2O) on compound formation and decomposition during pretreatment. In addition to these experiments, the readsorption of NO on decomposed $La(NO_3)_3$ was studied to verify the information of surface species observed during decomposition. NO was also adsorbed on La_2O_3 to compare the surface species formed and to follow the surface chemistry that occurred. Similar experiments were performed with CO_2 adsorption on La_2O_3 to probe the Lewis basicity of the surface. In addition to achieving a more complete understanding of the state of the catalysts, these data also provide a useful reference for further studies of NO decomposition and reduction over rare-earth oxides because carbonate and nitrate groups are likely to occur under reaction conditions. Infrared spectra taken under these various conditions have seldom been reported, and complete peak assignments are not found in the literature. To complement the DRIFTS experiments, which can be designed to be surface sensitive, XRD provided additional information on the bulk properties of the initial and pretreated samples and BET surface areas of the different samples were also measured.

2. Experimental Section

Three commercial La_2O_3 samples of different purity levels—Molycorp 99.9% (designated MC), Rhone-Poulenc 99.99% (designated RP), and Aldrich 99.999% (designated AL)—with the latter stored under N_2, were examined in their initial state and after an in situ pretreatment in the FTIR cell. This pretreatment consisted of 24 h at 300 K, 30 min at 403 K, and 30 min at 773 K, all under flowing Ar (MG Ind., UHP Grade) which was passed through a purifier (UOP Model P100) to reduce the contaminant level below 100 ppb. Furthermore, the influence of different calcination procedures on the RP La_2O_3 sample was examined. The "as-is" sample is noted by RP1, and identification of the different procedures is as follows: sample RP2, calcination at 1023 K for 10 h under flowing dry air (MG Ind., Grade 1, 50 cm^3/min); samples RP3, RP4, and RP5 calcined under flowing pure O_2 (MG Ind., UHP Grade) for 10 h at 1023 K (sample RP3), for 12 h at 1123 K (sample RP4), and for 12 h at 1273 K (sample RP5). Samples RP4 and RP5 were handled and stored in a N_2-purged drybox, except when the XRD experiments were conducted.

Commercial samples of $La_2(CO_3)_3$ (Aldrich, $La_2(CO_3)_3 \cdot 8H_2O$, 99.9%) and $La(NO_3)_3$ (Aldrich, $La(NO_3)_3 \cdot 6H_2O$, 99.99%) were used as is and were purged in situ in the FTIR system for 24 h under flowing Ar prior to taking spectra. $La_2(CO_3)_3$ was further pretreated in the DRIFTS cell in the same way as the La_2O_3 samples, but for the nitrate, a programmed thermal decomposition was performed under either flowing Ar or O_2. For adsorption experiments on the La_2O_3 samples or the decomposed nitrate, either a mixture of 4% NO in Ar (Matheson, certified) or CO_2 (MG Ind., UHP Grade, 99.99%) further diluted with Ar within the system was used.

The FTIR experiments were carried out with a Mattson Research Series 10000 FTIR equipped with an MCT narrow band detector (4000−750 cm^{-1}). Data collection and processing were performed with commercial Winfirst software. All spectra were taken at a resolution of 4 cm^{-1}. The spectrometer was also equipped with a diffuse reflection attachment (Harrick Scientific-DRA) that has been modified and connected to a gas supply system[22] to allow measurements under controlled atmospheres and temperatures (up to 800 K under flowing Ar). Spectra were taken under atmospheric pressure and an Ar flow of 30 sccm/min. To optimize the signal-to-noise ratio, 1000

(10) Bernal, S.; Botana, F. J.; García, R.; Rodríguez-Izquierdo, J. M. *React. Solids* **1987**, *4*, 23.
(11) Netzer, F. P.; Bertel, E. *Handbook on the Physics and Chemistry of Rare Earths*; Gschneidner, K. A., Jr., Eyring, L., Eds.; North-Holland: Amsterdam, 1982.
(12) Rosynek, M. P.; Magnuson, D. T. *J. Catal.* **1977**, *46*, 402.
(13) Rosynek, M. P. *Catal. Rev. Sci. Eng.* **1977**, *16*, 111.
(14) Rosynek, M. P; Magnuson D. T. *J. Catal.* **1977**, *48*, 417.
(15) Bernal, S.; Botana, F. J.; García, R.; Rodríguez-Izquierdo, J. M. *Thermochim. Acta* **1983**, *66*, 139.
(16) Capitán, M. J.; Centeno, M. A.; Malet, P.; Carrizosa, I.; Odrizosa, J. A.; Márquez, A.; Fernández Sanz, A. *J. Phys. Chem.* **1995**, *99*, 4655.
(17) Chu, Y.; Li, S.; Lin, J.; Gu, J.; Yang, Y. *Appl Catal. A* **1996**, *134*, 67.
(18) Bettmann, M.; Chase, R. E.; Otto, K.; Weber, W. H. *J. Catal.* **1989**, *117*, 447.
(19) Lacombe, S.; Zanthoff, H.; Mirodatos, C. *J. Catal.* **1995**, *155*, 106.
(20) Davydov, A. A.; Shepot?ko, M. L.; Budneva, A. A. *Kinet. Catal.* **1994**, *35*, 272.
(21) Davydov, A. A.; Shepot?ko, M. L.; Budneva, A. A. *Catal. Today* **1995**, *24*, 225.
(22) Mao, C.-F. and Vannice, M. A. *J. Catal.* **1995**, *154*, 230.

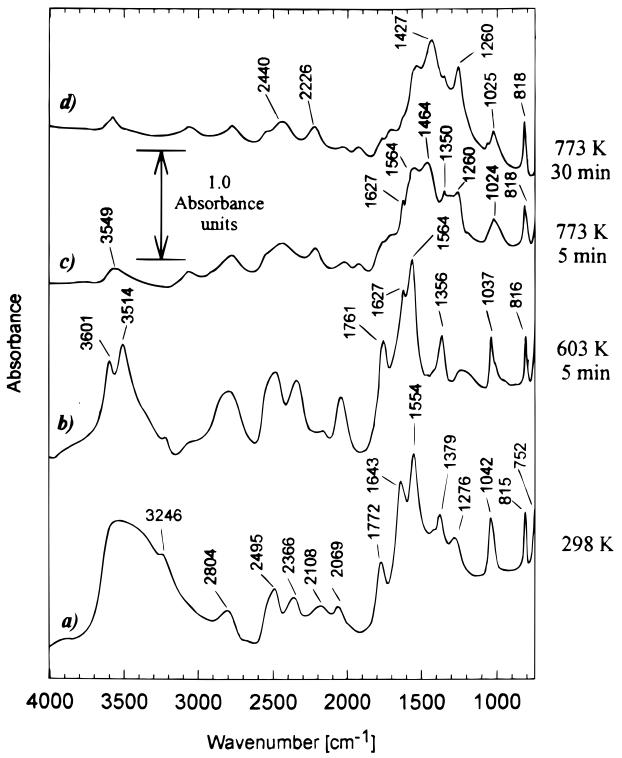

Figure 1. IR spectra of $La(NO_3)_3 \cdot 6H_2O$ (sample 1): (a) at 298 K prior to decomposition; (b) 5 min after reaching 603 K under flowing O_2; (c) 5 min after reaching 773 K under flowing O_2; (d) after 30 min at 773 K under flowing O_2. (All spectra referenced to KBr in Ar at the respective temperature.)

scans were added for one interferogram. The transformation into absorbance spectra was carried out by using background spectra collected under identical conditions with KBr powder in the holder. For spectra at temperatures different from 298 K, a corresponding background spectrum with KBr was used to correct for the influence of temperature. It needs to be noted that, in general, diffuse reflectance spectra taken at higher temperatures will exhibit line broadening, peak shifts, and a decrease in intensity. Thus, comparison of spectra obtained at different temperatures has to be performed cautiously.

XRD measurements were performed with either a Rigaku Geigerflex diffractometer equipped with a Dmax-B controller, or a Scintag VAX 3100 System. In both cases spectra were obtained with Cu Kα radiation (1.5405 Å). BET surface area measurements were carried out with a Quantasorb system using three premixed gases containing 10, 20, and 30% N_2 in He (99.999%).

3. Results

3.1. Characterization and Decomposition of Hydrated Lanthanum Nitrate. The spectrum of commercial $La(NO)_3 \cdot 6H_2O$ was taken after purging the sample with Ar in the DRA cell for 24 h at 300 K and is shown in Figure 1a. Table 1 lists the different peaks and their assignments based on earlier studies.[23−27] Three regions of vibrational modes can be distinguished: 3650−3000 cm^{-1} (OH vibrations), 3000−1700 cm^{-1} (combination and overtone modes of nitrate vibrations), and 1650−750 cm^{-1} (nitrate vibrations). The nitrate ion (point group D_{3h}) gives four vibrations: υ_1 (NO stretch), υ_2 (out-of-plane), and the two doubly degenerate vibrations υ_3 (NO_2 stretch) and υ_4 (NO_2 bend). Going from the nitrate ion to either a unidentate or bidentate coordinated nitrate group lowers the symmetry to C_{2v} and leads to a splitting of the degenerate vibrations, each into two frequencies. To prevent confusion, Table 1 also summarizes the assignments of vibrational modes and the nomenclature generally used in the literature for the different types of nitrate species.[25] The spectrum of $La(NO_3)_3$ shows a number of peaks in the NO_2 stretching region (1650−1250 cm^{-1}), suggesting the presence of nitrate ions with C_{2v} symmetry because of the observed splitting of bands. Assignments for unidentate species and bidentate groups can be made. As most of the peaks are rather broad, overlapping signals are probably involved thus justifying the assignment of the peaks to both coordinative species. In addition, $\delta(H_2O)$ vibrations of lattice-coordinated water, and possibly adsorbed water, are observed in the latter region. The assignment of overtones and combination vibrations was performed according to Gatehouse et al.[28]

The BET surface area of $La(NO_3)_3 \cdot 6H_2O$ was 0.25 m^2/g (Table 2). It was not possible to measure the surface area after an in situ pretreatment because $La(NO_3)_3 \cdot 6H_2O$ melts at 40 °C. The decomposition of lanthanum nitrate in the DRIFTS cell was studied under two different conditions. The first sample was heated under flowing oxygen (99.99%, 10 cm^3/min) with the following temperature profile: heat at 10 K/min to 403 K, hold 30 min, heat at 10 K/min to 773 K, hold 2 h, cool to room temperature. The sample subsequently was heated again at 773 K for 2 h in pure Ar (25 cm^3/min). The thermal treatment of sample 2 was the same with the exception that pure Ar was used in both heating cycles.

Figure 1 depicts spectra of hydrated $La(NO_3)_3$ taken at 298 K (Figures 1a), 603 K (taken while heating to 773 K, Figure 1b), and at 773 K under flowing oxygen (sample 1, Figure 1c,d). At 603 K the most significant change occurs in the region of OH vibrations: the broad band between 3700 and 3200 cm^{-1} is resolved into two peaks at 3601 and 3514 cm^{-1}, the peak at 1643 cm^{-1} loses intensity, and a previously hidden peak is visible at 1627 cm^{-1}. Dehydration of the sample starts at 403 K (not shown), and peaks representing surface OH groups are now visible, and upon reaching 773 K, only a weaker, very broad feature around 3549 cm^{-1} is left. Substantial changes also occur in the region of the nitrate group frequencies. The intense peak at 1761 cm^{-1} is almost lost (shifted from 1772 cm^{-1} in initial spectrum a) and signals at 1627, 1564, and 752 cm^{-1} decrease in intensity. The band at 1379 cm^{-1} in the initial sample shifts to 1350 cm^{-1}, new bands at 1464 and 1260 cm^{-1} develop, and the peak around 1024 cm^{-1} (shifted from 1042 cm^{-1}) is broadened. After 30 min at 773 K (Figure 1d) significant peaks remain at 1427, 1260, 1025, and 818 cm^{-1}. New maxima in the region for combination bands and overtones are now found at 2440 ($2\upsilon_1$ at 1260 cm^{-1}) and 2226 cm^{-1} ($\upsilon_4 + \upsilon_6$ at 1427 and 818 cm^{-1}). No further changes occur during heating for a total of 2 h (not shown). The state of sample 1

(23) Ferraro, J. R. *J. Mol. Spectrosc.* **1960**, *4*, 99.
(24) Vratny F. *Appl. Spectrosc.* **1959**, *13*, 59.
(25) Addison, C. C.; Simpson, W. B. *J. Chem. Soc.* **1965**, 598.
(26) Addison, C. C.; Gatehouse, B. M. *J. Chem. Soc.* **1960**, 613.
(27) Nakamoto, K. *Infrared and Raman Spectra of Inorganic and Coordination Compounds*, 4th ed.; John Wiley & Sons: New York, 1986.
(28) Gatehouse, B. M.; Comyns, A. E. *J. Chem. Soc.* **1958**, 3965.

Table 1. Vibrational Mode Identification for $La(NO_3)_3 \cdot 6H_2O$ DRIFT Spectra Based on Previous IR Peak Assignments[23−27a]

assignment for point group D_{3h}	assignment for point group C_{2v} unidentate species	assignment for point group C_{2v} bidentate species
Nitrate Group Vibrations (cm^{-1})		
N═O stretch ν_1	N═O str ν_1 1042 s	N═O str ν_1 covered by intense 1643 (δ H_2O)
out-of-plane ν_2	out-of-plane ν_6 815 sp, s	out-of-plane ν_6
	NO_2 str sym ν_1 1276 m, b	NO_2 str sym ν_2 1042 s
NO_2 stretch ν_3	NO_2 str asym ν_4 1554 vs	NO_2 str asym ν_4 1379 m
	NO_2 bend sym ν_3 752 sp, s	NO_2 bend sym ν_3
NO_2 bend ν_4	NO_2 bend asym ν_5	NO_2 bend ν_5 752 sp, s
Combination and Overtone Vibrations of Nitrate Group (cm^{-1})		
unidentate		bidentate
$2\nu_1$ 2495 b, m		$2\nu_4$ 2804 b, m
$\nu_4 + \nu_6$ 2366 b, m		
$\nu_1 + \nu_6$ 2108 b, m		
$2\nu_2$ 2069 b, m		
$\nu_2 + \nu_6$ 1772 m		
Hydroxyl Group Vibration (cm^{-1})		
OH, water of hydration		3700−3200 s, vb 3246 sh (ν OH), 1643 s (δ H_2O)

[a] Abbreviations: vs very strong, s strong, m medium, w weak, vw very weak, b broad, sp sharp, sh shoulder.

Table 2. BET Surface Areas of the $La(NO_3)_3 \cdot 6H_2O$, $La_2(CO_3)_3 \cdot 8H_2O$, and Various La_2O_3 Samples after Different Pretreatments, Listed with Pretreatment Conditions and Abbreviations Used for the Samples in the Text

compound and pretreatment	BET surface area in m^2/g
$La(NO_3)_3 \cdot 6H_2O$ as is	0.25
$La_2(CO_3)_3 \cdot 8H_2O$ as is	3.32
La_2O_3 (Molycorp 99.9%) as is, MC	4.62
La_2O_3 (Aldrich 99.999%) as is, stored in drybox, AL	1.14
La_2O_3 (Rhone-Poulenc 99.99%) as is, RP1	3.0
La_2O_3 (Rhone-Poulenc 99.99%) calcination 10 h at 1023 K in air, RP2	4.7
La_2O_3 (Rhone-Poulenc 99.99%) calcination 10 h at 1023 K in O_2, RP3	3.9
La_2O_3 (Rhone-Poulenc 99.99%) calcination 12 h at 1123 K in O_2, stored in drybox, RP4	0.71
La_2O_3 (O_2-Poulenc 99.99%) calcination 12 h at 1273 K in O_2, stored in drybox, RP5	0.87

after the first thermal treatment and further development during the second treatment in pure Ar are compared in Figure 2a,b. At 298 K small peaks are still observed at 1637 and 1592 cm^{-1}, but the most intense signals are at 2250, 1444, 1389, 1351, 1280, 1030, and 824 cm^{-1}. After the second heating cycle in pure Ar (Figure 2b), the intensity of the peaks at 2250, 1637, 1592, and 1280 cm^{-1} decreases, the 1444 cm^{-1} feature is still prominent and shifted to 1450 cm^{-1}, the peak at 1351 cm^{-1} appears now at 1363 cm^{-1}, and the signal at 1389 cm^{-1} is still visible as a shoulder. New peaks grow in at 1062 and 778 cm^{-1} together with combination bands at 2390 and 1770 cm^{-1}. In the OH frequency region only small peaks at 3577 and 3539 cm^{-1} remain.

The behavior of the second sample, which was heated in pure Ar, was identical to that under O_2 up to 773 K. Figure 3 shows the spectra at 603 and 773 K at different stages of the decomposition. As with the sample heated in O_2, sudden changes occur when 773 K is reached (Figure 3b). The peaks at 1760, 1620, and 1567 cm^{-1} (shifted to 1542 cm^{-1}) again decrease significantly, new species at 2435, 2218, 1436, and 1253 cm^{-1} grow in, and the peak at 1030 cm^{-1} decreases and shifts to 1021 cm^{-1} with a shoulder at 1064 cm^{-1}. The peak at 1350 cm^{-1} becomes less broad, and the signal at 805 cm^{-1} shifts to 818 cm^{-1}. The OH region shows only a small peak at 3575 cm^{-1}. While these characteristics do not change a lot in the case of heating in oxygen, drastic modifications are observed for the heating sequence in Ar. As shown in Figure 3c, the intense peak at 1253 cm^{-1} starts to decrease after 1 h at 773 K and shifts to 1250 cm^{-1}, the shoulder at 1064 cm^{-1} develops into a small peak,

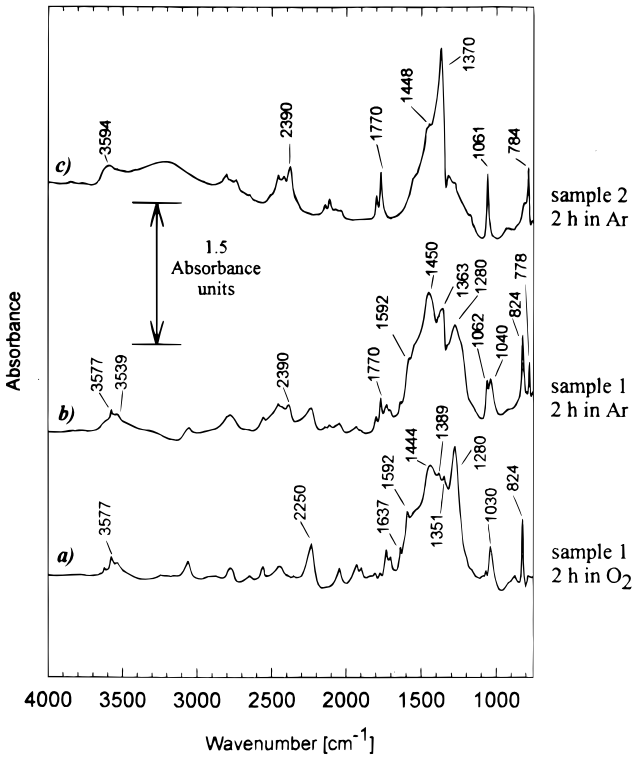

Figure 2. IR spectra of $La(NO_3)_3$ at 298 K after the decomposition cycle: (a) sample 1 after 2 h decomposition under flowing O_2 at 773 K; (b) after subsequent decomposition for 2 h under flowing Ar at 773 K; (c) sample 2 after 2 h decomposition at 773 K exclusively under Ar. (All spectra referenced to KBr in Ar at 298 K.)

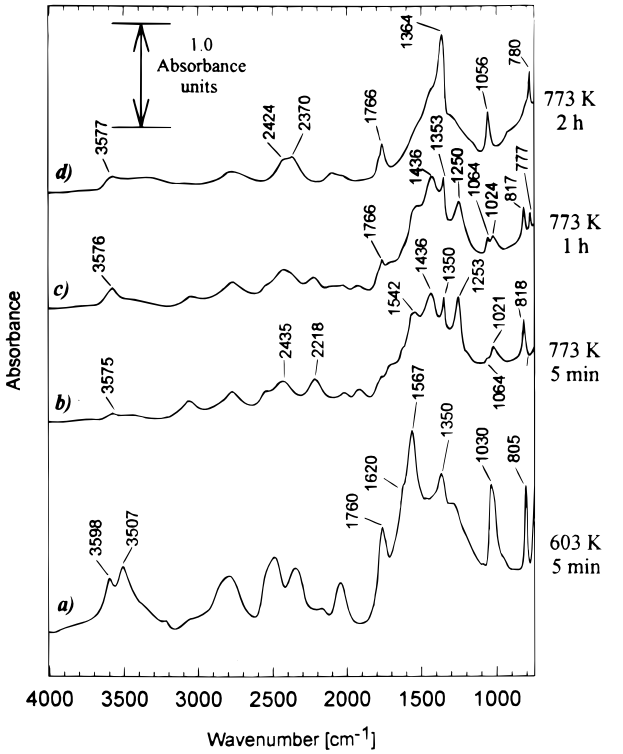

Figure 3. IR spectra of $La(NO_3)_3 \cdot 6H_2O$ (sample 2) during decomposition under flowing Ar: (a) 5 min after reaching 603 K; (b) 5 min after reaching 773 K; (c) after 1 h at 773 K; (d) after 2 h at 773 K. (All spectra referenced to KBr in Ar at the respective temperature.)

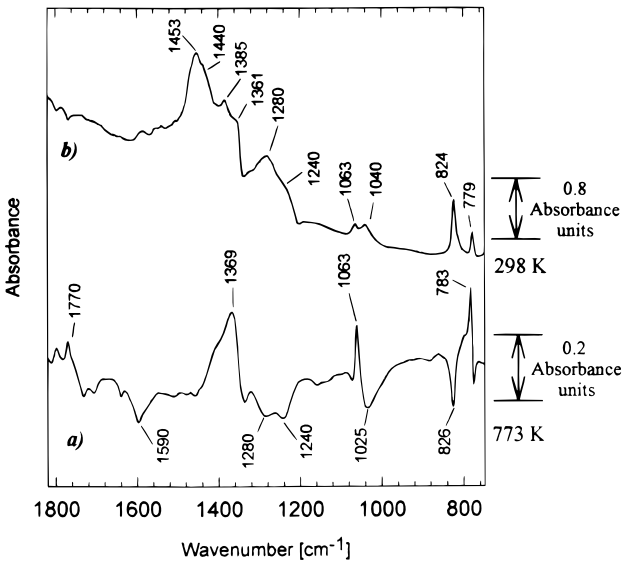

Figure 4. IR spectra after flowing 4% NO in Ar over sample 1 (after decomposition) for 30 min: (a) at 773 and (b) 298 K. (Each spectrum referenced to that just prior to NO adsorption at 773 or 298 K, respectively.)

and new bands are found at 1766 and 777 cm^{-1}. After 2 h at 773 K, the only prominent, sharp peaks are found at 2370, 1766, 1364, 1056, and 780 cm^{-1}. The peak at 1364 cm^{-1} exhibits broad shoulders, so the bands around 1436 and 1542 cm^{-1} are supposedly still present at low intensity. No further changes were observed after a second heating cycle. As already mentioned, Figure 2 compares the spectrum at 298 K of sample 1 after one heating cycle in oxygen with that of sample 2 after the first thermal treatment in Ar. The latter spectrum (Figure 2c) has the same peak structure as the one taken at 773 K, with peaks at 3594, 2390, 1770, 1448, 1370, 1061, and 784 cm^{-1}. Table 3 summarizes the peaks, their development during the decomposition, and their assignments.[25−27,29−31] It is noted that shifts in the peak wavenumbers occur due to temperature if peak positions at 773 and 298 K are compared. Overlapping assignments may occur. Table 4 shows schematic diagrams of the different NO_x species.

Adsorption of NO was performed on sample 1 following decomposition to compare any new species with intermediates observed during decomposition. Data were collected after adsorption at 298 and 773 K, and the respective spectra are shown in Figure 4. Exposure to 4% NO at 298 K for 30 min led to an increase in intensity at 1453, 1440 (shoulder), 1385, 1361 (shoulder), 1280, 1240 (shoulder), 1063, 1040, 824, and 779 cm^{-1} (Figure 4b). However, the identical procedure performed at 773 K resulted in the growth of bands at 1770, 1369, 1063, and 783 cm^{-1} (Figure 4a), while losses around 1590, 1280−1240, 1025, and 826 cm^{-1} indicate that the concentrations of other species present at the surface decreased. Assignments for the peaks that develop are also included in Table 3.

The XRD patterns for the as-is $La(NO_3)_3 \cdot 6H_2O$ sample and for both decomposed samples are depicted in Figure 5. Peak assignments are based on standard reference data.[6,32] Most of the nitrate has decomposed to La_2O_3; however, some peaks have to be assigned to different compounds. An intense study of available files[32] shows that both samples contain small amounts of $La(OH)_3$, but only sample 1 (Figure 5b) is likely to contain $LaONO_3$.

3.2. Characterization of Hydrated Lanthanum Carbonate. DRIFT spectra were taken of the initial commercial $La_2(CO_3)_3 \cdot 8H_2O$ material and the sample after an in situ pretreatment cycle as performed with the oxide samples (see Experimental Section). Both spectra are depicted in Figure 6 (a and b), while Figure 7 shows the XRD spectra and their peak assignments.[32] Table 5 describes the assignments for the IR data.[9,10,33−35] The assignments for the vibrational modes of the CO_3^{2-} ion follow the nomenclature for the nitrate ion in section 3, as both belong to the same point groups, i.e., D_{3h} in ionic binding and C_{2v} in coordinated binding states (see Table 1). For the IR spectra, the most significant change during the pretreatment occurs in the region of OH vibrations, as the broad peak between 3600 and 2700 cm^{-1} is replaced by single peaks at 3630, 3616, and 3484 cm^{-1}. New peaks are observed at 2899, 2186, 1824, 1757, 1370, and 844 cm^{-1}, whereas other peaks shift slightly (2525, 2347, 1608, 1481, 1083, and 861 cm^{-1}). The XRD spectrum of the initial carbonate exhibits a low signal-to-noise ratio and broad, weak peaks, which is most likely due to the large amount of

(29) Bünzli J.-C. G.; Moret E.; Yersin J.-R. *Helvet. Chim. Acta* **1978**, *61*, 762.
(30) Davydov, A. A.; Rochester, C. H. *Infrared Spectroscopy of Adsorbed Species on the Surface of Transition Metal Oxides*; John Wiley & Sons: Chinchester, 1984.
(31) Patil K. C; Gosavi R. K; Rao, C. N. R. *Inorg. Chim. Acta* **1967**, *1*, 155.
(32) *International Powder Diffraction File*; Centre for Diffraction Data of Philadelphia: 1991.
(33) Goldsmith, J. A.; Ross, S. D. *Spectrochim. Acta* **1967**, *23A*, 1967.
(34) Caro, P. E.; Sawyer, J. O.; Eyring, L. *Spectrochim. Acta* **1972**, *28A*, 1167.
(35) Dexpert H.; Antic-Fidancev, E.; Coutures, J. P.; Caro, P. *J. Cryst. Spectrosc. Research* **1982**, *12*, 129.

Table 3. Vibrational Mode Identification for Species Observed during Decomposition of $La(NO_3)_3$ (Sample 1, *Sample 2*) and after NO Adsorption on Sample 1 after Decomposition

experimental conditions	peak position (cm^{-1}) and vibrational mode
603 K in O_2	1761m $\nu_2 + \nu_{5/3}$, 1627s ν_1, 1564s ν_4, 1356m $\nu_{4/1}$, 1037m ν_2, 816m ν_6 unidentate and bidentate nitrate NO_3^-
603 K in Ar	*1620*m,sh ν_1, *1567*s ν_4, *1350*m ν_4, *1030*m ν_2, *805*m ν_6 unidentate and bidentate nitrate NO_3^-
773 K in O_2 (30 min)	2440w $2\nu_1$, 2226w, 1427s ν_4, 1260s ν_1, 1025m ν_2, 818m ν_6 oxynitrate
773 K in Ar (5 min)	*2435*w $2\nu_1$, *2218*w $\nu_4 + \nu_6$, *1436*s ν_4, *1253*s ν_1, *1021*w ν_2, *818*m ν_6 oxynitrate
773 K in Ar (2 h)	*2370*m $\nu_3 + \nu_1$, *1766*m $\nu_1 + \nu_4$, *1364*m ν_3, *1056*m ν_1, *780*m ν_2 ionic nitrate
298 K after decomposition	1637w ν_1, 1592w ν_4, 1351w $\nu_{4/1}$ unidentate and bidentate nitrate NO_3^- 2250w $\nu_4 + \nu_6$, 1444−1450m ν_4, 1280m ν_1, 1030−1040m ν_2, 824m ν_6 oxynitrate 2390w $\nu_3 + \nu_1$, 1770w $\nu_1 + \nu_4$, 1363m ν_3, 1062m ν_1, 778w ν_2 *2390*m $\nu_3 + \nu_1$, *1770*m $\nu_1 + \nu_4$, *1370*s ν_3, *1061*m ν_1, *784*m ν_2 ionic nitrate
298 K NO adsorption	1453s ν_4, 1280m ν_1, 1040w ν_2, 824m ν_6 oxynitrate 1385s ν_3, 1063w ν_1, 779w ν_2 ionic nitrate 1440sh $\nu_{N=O}$, 1361sh ν_{as}, 1240 sh ν_{sym} nitrito and nitro groups NO_2^-
773 K NO adsorption	1770w $\nu_1 + \nu_4$, 1369m ν_3, 1063m ν_1, 783m ν_2 ionic nitrate

Table 4. Schematic Configuration Geometry of Nitrate and Nitrite Groups

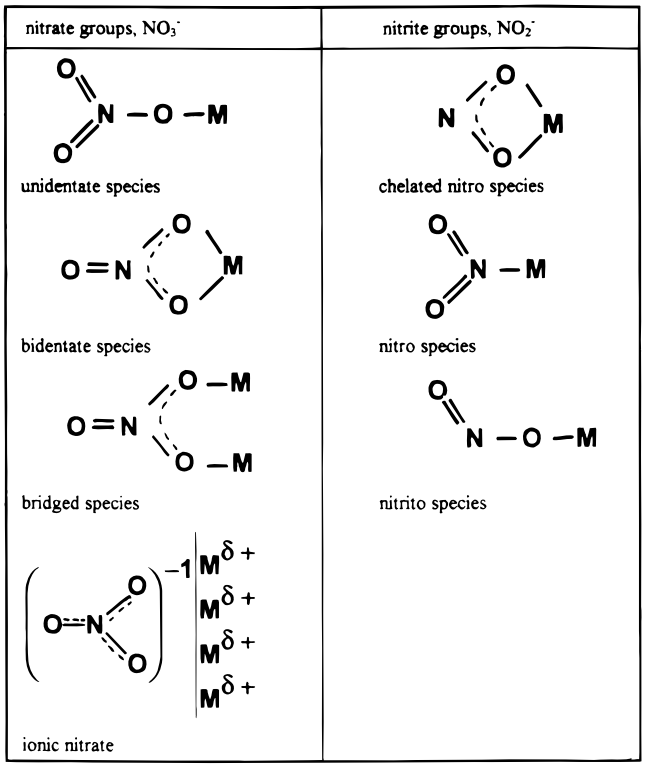

adsorbed water on this highly hygroscopic material. A comparison with XRD patterns reported in the literature does not reveal any similarities; however, after pretreatment, the quality of the XRD spectrum was improved and peak assignments are possible.[32] The BET surface area of the carbonate after the in situ pretreatment was 3.32 m^2/g, as listed in Table 2.

3.3. Characterization of Lanthanum Oxide. Seven samples of La_2O_3 were examined—three as is (MC, AL, RP1) and four (RP2-RP5) after being treated by one of the different calcination procedures as described in the Experimental Section, and they were characterized by DRIFTS and XRD. The spectra given

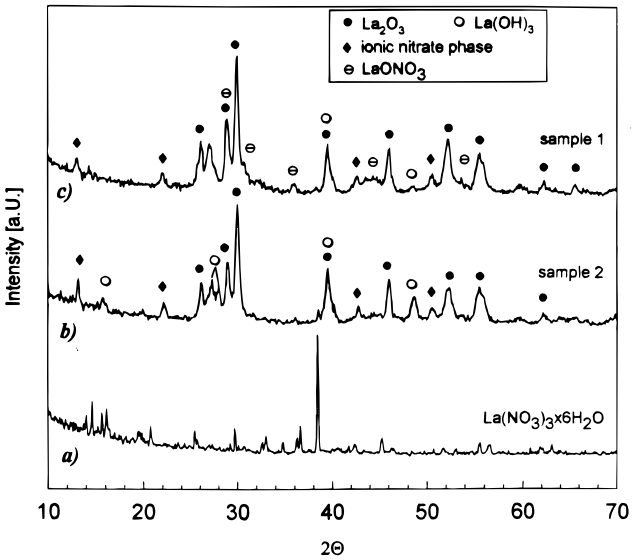

Figure 5. XRD pattern of (a) $La(NO_3)_3 \cdot H_2O$ as is, (b) $La(NO_3)_3$ after decomposition for 4 h at 773 K under flowing Ar (sample 2), and (c) $La(NO_3)_3$ after decomposition for 2 h under flowing O_2 and 2 h under flowing Ar at 773 K (sample 1).

in Figure 6c,d (sample MC) and 6,f (sample AL) show the effect of an in situ pretreatment (30 min at 403 K, 30 min at 773 K), whereas Figure 8 compares the effect of different calcination processes (RP1−RP3, RP5; spectra taken prior to the in situ pretreatment). The corresponding XRD patterns (prior to the in situ pretreatment) with peak assignments are shown in Figure 9 for all samples.[6,32] (Sample RP1 is not shown as its pattern is identical with sample MC.) The IR and XRD spectra of sample RP4 (12 h at 1123 K) are also not shown as they are identical with those for sample RP5 (12 h at 1273 K). The peak positions and assignments of the IR data are summarized in Table 5.[27,35−37] The BET surface areas of all samples are listed in Table 2.

(36) Turcotte, R. P.; Sawyer J. O.; Eyring L. *Inorg. Chem.* **1969**, *8*, 238.

(37) Zubova N. V.; Makarov, V. M.; Nikol'skii, V. D.; Petrov, P. N.; Teterin, E. G.; Chebotarev, N. T. *Russ. J. Inorg. Chem.* **1968**, *13*, 7.

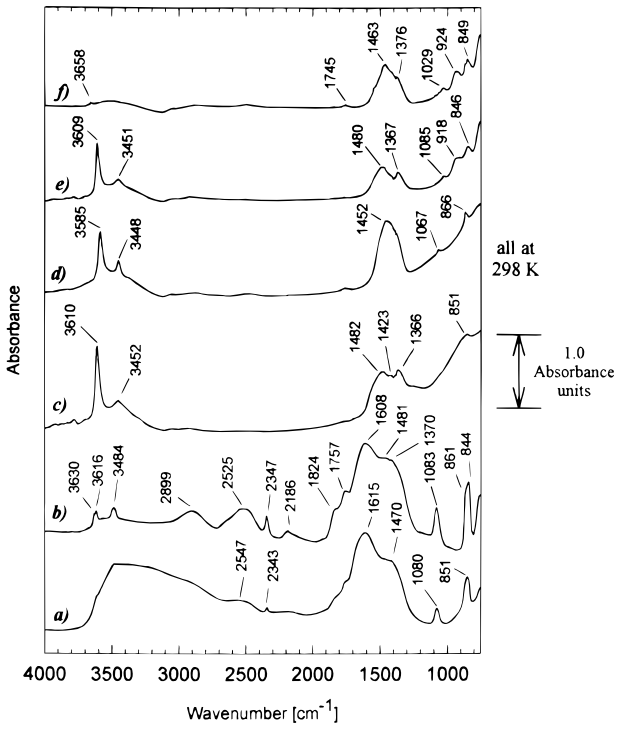

Figure 6. IR spectra at 298 K of (a) $La_2(CO_3)_3 \cdot 8H_2O$ as is, (b) $La_2(CO_3)_3$ after in situ pretreatment of 30 min at 773 K under Ar, (c) La_2O_3 (sample MC) as is, (d) La_2O_3 (sample MC) after in situ pretreatment of 30 min at 773 K, (e) La_2O_3 (sample AL) as is, and (f) La_2O_3 (sample AL) after in situ pretreatment of 30 min at 773 K. (All spectra referenced to KBr in Ar at 298 K.)

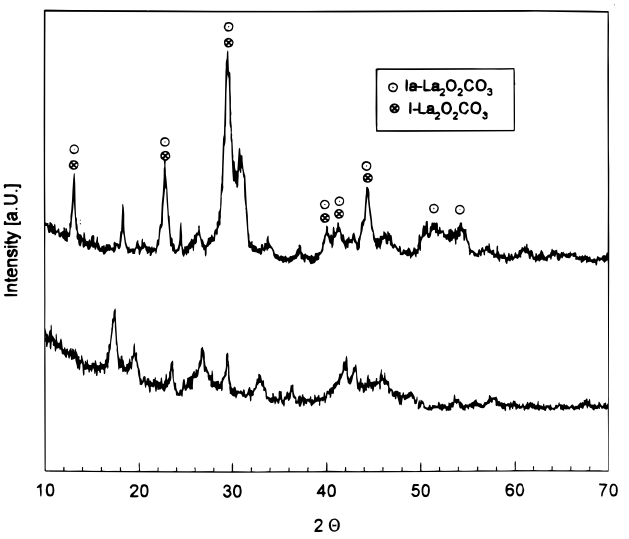

Figure 7. XRD pattern of (a) $La_2(CO_3)_3 \cdot 8H_2O$ as is, and (b) $La_2(CO_3)_3$ after in situ pretreatment of 30 min at 773 K under Ar.

The in situ pretreatment of sample MC (Figure 6c,d) results in a peak shift in the OH region from 3610 and 3452 cm^{-1} to 3585 and 3448 cm^{-1}, respectively, the three peaks at 1482, 1423, and 1366 cm^{-1} collapse into one broad peak at 1452 cm^{-1}, a new peak occurs at 1067 cm^{-1}, and the weak signal at 851 cm^{-1} develops into a small peak at 866 cm^{-1}. For sample AL (Figure 6e,f), the peaks at 3609 and 3451 cm^{-1} are lost and only a very weak signal remains at 3658 cm^{-1}, while all other peaks shift by various extents and a very weak peak occurs at 1745 cm^{-1}. The spectra after different calcination procedures (Figure 8a−d) show very similar peak positions in the OH region (around 3610 and 3450 cm^{-1}) except for spectrum d (sample RP5), which has only a very weak signal at 3651 cm^{-1}. In the region below 1600 cm^{-1}, spectra a and c show peaks of comparable position and shape (around 1480, 1360, and 850 cm^{-1}), whereas spectrum d exhibits a weaker, broad peak at 1483 cm^{-1}, with shoulders at 1540 and 1401 cm^{-1}, and additional peaks at 1030, 943, and 925 cm^{-1}. In contrast, spectrum b shows intense signals at 1507, 1466, and 1405 cm^{-1}, sharp peaks at 1824, 1748, 1084, and 857 cm^{-1}, and a broader 2501 cm^{-1} peak.

The adsorption of CO_2 was performed at 298 and 773 K on sample RP5 by flowing 10% CO_2 in Ar, and Figure 10 shows the carbonate vibration region of the respective DRIFT spectra. Spectrum a was taken after a 30-min exposure to CO_2 at 298 K. A broad peak grows in at 1623 cm^{-1} with a shoulder at 1569 cm^{-1}, and other broad features of varying intensity are visible at 1329, 1280, 1206, 1036, and 842 cm^{-1}. A subsequent heating cycle identical with the sample pretreatment procedure was performed, and the resulting spectrum is shown in Figure 10b. It depicts new bands at 1783, 1731, 1559 (with a shoulder at 1502 cm^{-1}), 1382, 1060, 1052, 876, 863, and 860 cm^{-1}. Figure 10c shows the spectrum taken after 30 min of exposure to CO_2 at 773 K. Broad peaks are found at 1505, 1356, 1075, 1055, and 844 cm^{-1}. After subsequently cooling to 298 K, the spectrum obtained is depicted in Figure 10d. As expected for the temperature effect, the peaks are now narrower, the positions are shifted to 1517, 1363, 1061, and 846 cm^{-1}, and additional peaks are found at 1780, 1727, 1449, and 872 cm^{-1}. The assignments for the different peaks are included in Table 5.[27,38]

NO adsorption at 298 and 773 K on sample RP5 was conducted by flowing 4% NO in Ar for 30 min, and Figure 11 shows the respective DRIFTS spectra of the nitrate vibration region. After exposure to NO at 298 K, a prominent peak is found at 1149 cm^{-1} together with smaller peaks at 1697, 1610, 1412, 1300, 1004, and 818 cm^{-1}, and the intense signals of gas-phase NO and N_2O (an impurity in the NO) are visible. In contrast, the spectrum taken at 773 K reveals the gas-phase spectra of NO, CO_2, and N_2O, the latter with a shoulder at 2173 cm^{-1} representing adsorbed N_2O, a peak at 1522 cm^{-1}, and intensity losses at 1415 and 1285 cm^{-1}. Peak positions and assignments are listed in Table 6.[27,30,39]

4. Discussion

4.1. Lanthanum Nitrate and NO Adsorption. The results of previous studies on the decomposition of $La(NO_3)_3$ will be compared with those presented here; therefore, a brief summary of this prior work is provided. Wendlandt[40] pyrolyzed $La(NO_3)_3 \cdot 6H_2O$ in a thermobalance under flowing air to examine its decomposition and observed a loss of water of hydration starting at 323 K. The monohydrate was formed at 443 K and was stable up to 513 K, where it started to form the anhydrous salt, $La(NO_3)_3$. This compound decomposed by losing nitrogen oxides starting at 693 K, which resulted in the formation of $LaONO_3$. Finally, the

(38) Gatehouse, B. M.; Livingstone, S. E.; Nyholm, R. S. *J. Chem. Soc.* **1958**, 3137.
(39) Cerruti, F.; Modone, E.; Guglielminotti E.; Borello E. *Faraday Trans.* **1974**, *70*, 729.
(40) Wendlandt, W. W. *Anal. Chim. Acta* **1956**, *15*, 435.

Table 5. Vibrational Mode Identification of $La_2(CO_3)_3 \cdot 8H_2O$, Various La_2O_3 Samples, and after CO_2 Adsorption at 298 and 773 K on La_2O_3 (Sample RP5)[a]

	hydroxyl group vibrations (cm^{-1})[1]			combination and overtone vibrations (cm^{-1})	carbonate group vibrations (cm^{-1})			
	isolated OH	$La(OH)_3$	La(O)OH		bulk CO_3^{2-}	$La_2O_2CO_3$ I, Ia, II	unidentate CO_3^{2-}	bidentate CO_3^{2-}
$La_2(CO_3)_3 \cdot 8H_2O$		3600−2700 s,vb[2]		2547vb,[6] 2343w[7]	1615s,[3] 1470sh,[11] 1080m,[13] 851m[14]			
after in situ pretreatment	3630w,sh,	3616w	3484w[4]	2899bw,[5] 2525vb,w,[6] 2347sp,w,[7] 2186vw,[8] 1824sh,[9] 1757sh[10]		1608vs,vb 1481 vs I Ia,[11] 1370 sh,s Ia,[12] 1083m Ia,[13] 861sh 844s I[14]		
La_2O_3 (MC)		3610s	3452m				1482s 1423sh,[11] 1366s,[12] 851w[14]	
La_2O_3 (MC) after in situ pretreatment			3585s, 3448m				1452s,[11] 1067w,[13] 866w[14]	
La_2O_3 (AL)		3609s	3451m	918w[15]			1480m,[11] 1367m,[12] 1085w,[13] 846w[14]	
La_2O_3 (AL) after in situ pretreatment	3658vw			1754vw,[10] 924w[15]			1463m,[11] 1376m,[12] 1029w,[13] 849w[14]	
La_2O_3 (RP1)		3611s	3452m				1483s,[11] 1366s[12]	
La_2O_3 (RP2)		3609s	3448m	2501b,[6] 1824w,[9] 1748w[10]		1507vs,[11] 1466vs,[11] 1405sh,[12] 1084m,sp,[13] 857m[14]		
La_2O_3 (RP3)		3608s	3452m				1479s,[11] 1364s,[12] 849w[14]	
La_2O_3 (RP5)	3651w			943s 925s[15]			1483m, 1401sh,w,[11] 1384sh,w[12]	1540sh,vw,[12] 1030m,[13] 843s[14]
CO_2 adsorption on La_2O_3 (RP5) 298 K								1623m, 1569sh,m,[12] 1329w, 1280sh, 1206w,[11] 1036w,[13] 842vw[14]
after heating to 773 K, taken at 298 K				1783m 1731m[9]			1559m, 1502sh,[11] 1382m,[12] 1060w, 1052w,[13] 876w, 863w 860w[14]	
CO_2 adsorption on La_2O_3 (RP5)								
773 K							1505s,[11] 1356s,[12] 1075w, 1055w,[13] 844w[14]	
298 K				1780m 1727m[9]			1517s, 1449m,[11] 1363s,[12] 1061m,[13] 872m, 846m[14]	

[a] Key: ν OH; [2]assignment different from listing in table: ν OH water of hydration; [3]overlay with intense δ H_2O for water of hydration; [4]assignment different from listing in table: ν OH for $LaCO_3OH$; [5]$2\nu_4$; [6]$\nu_4 + \nu_2$; [7]$\nu_4 + \nu_6$; [8]$2\nu_2$; [9]$\nu_2 + \nu_3$; [10]$\nu_2 + \nu_5$; [11]ν_4; [12]ν_1; [13]ν_2; [14]ν_6; [15]combination of La−O fundamental modes.

Table 6. Vibrational Mode Identification after NO Adsorption at 298 and 773 K on La_2O_3 (Sample RP5)[a]

	gas-phase species vibrations (cm^{-1})			NO_3^- vibrations (cm^{-1})		NO_3^- vibration (cm^{-1})	NO^- ($N_2O_2^{2-}$) vibration (cm^{-1})	CO_3^{2-} vibration (cm^{-1})
	CO_2	N_2O	NO	bidentate/bridged	unidentate	nitro		losses
NO adsorption at 298 K		2236	1904	1697w, 1610m, 1300w,[2] 1004w[3]		1412w,[4] 1300w,[5] 817w[6]	1149s,b[7]	
NO adsorption at 773 K	2363	2236, 2173[8]	1909		1522m[2]			1415, 1285

[a] Key: [1]ν_1; [2]ν_4; [3]ν_2; [4]ν_{as}; [5]ν_{sym}; [6]δ_{NO_2}; [7]ν_{NO}; [8]N_2O_{ads}.

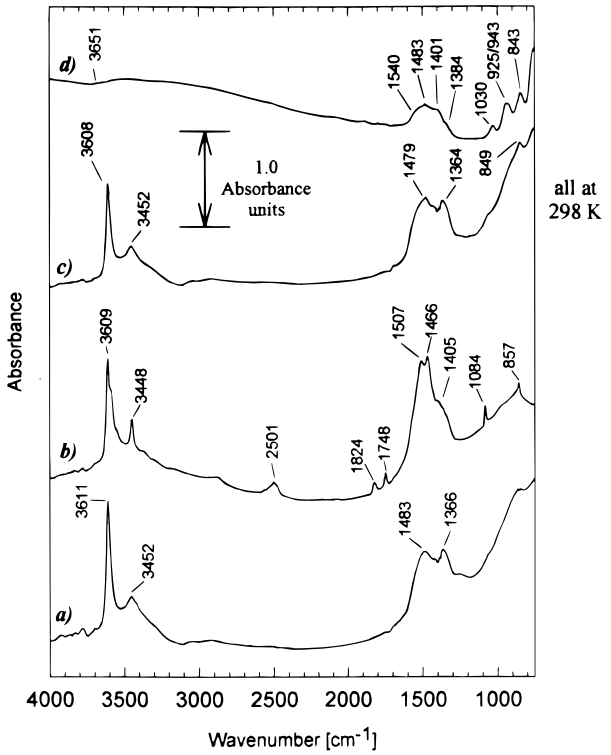

Figure 8. IR spectra at 298 K of La_2O_3: (a) sample RP1, as is; (b) sample RP2, calcined at 1023 K under air for 10 h; (c) sample RP3, calcined at 1023 K under O_2 for 10 h; (d) sample RP5, calcined at 1273 K under O_2 for 12 h. (All spectra referenced to KBr in Ar at 298 K.)

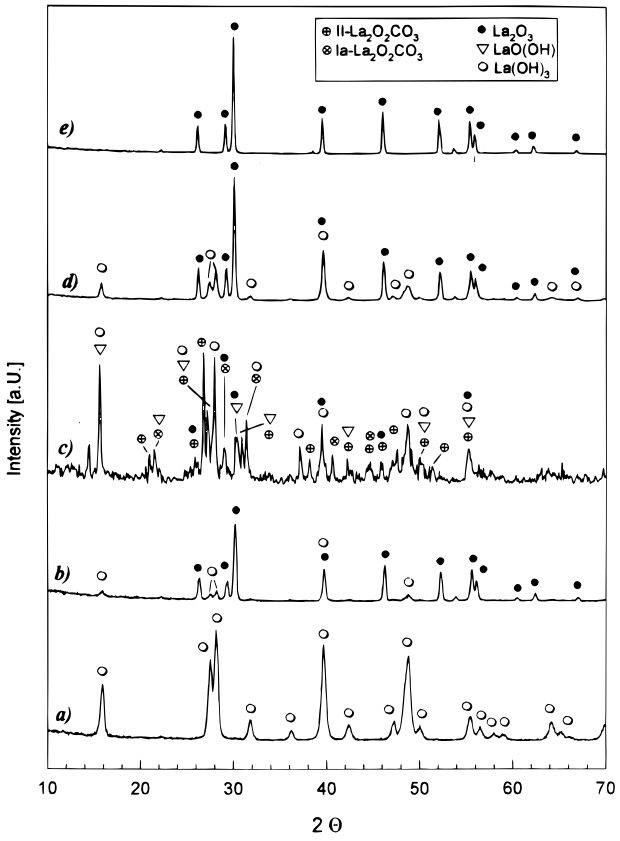

Figure 9. XRD patterns for (a) La_2O_3 (sample MC) as is, (b) La_2O_3 (sample AL) as is, (c) La_2O_3 (sample RP2), calcined at 1023 K under air for 10 h, (d) La_2O_3 (sample RP3), calcined at 1023 K under O_2 for 10 h; and (e) La_2O_3 (sample RP5), calcined at 1273 K under O_2 for 12 h.

oxynitrate started to decompose at 848 K to form La_2O_3 at 1053 K. Patil et al.[31] reported that the decomposition of $La(NO_3)_3 \cdot 6H_2O$ under vacuum produced three compounds: anhydrous $La(NO_3)_3$ (513−693 K), oxynitrate (788−848 K), and lanthanum oxide, whose formation started at 1003 K. IR peak positions for intermediate oxynitrates (1600, 1449, 1365, 1333, 1308, 1206, 1030, 818, 707 cm^{-1}) were listed by the authors and compared with those for $La(NO_2)_3$. It was concluded that nitrites were not formed as an intermediate in the decomposition of $La(NO_3)_3$.[31] Bünzli et al. also reported IR data for $LaONO_3$, and anhydrous nitrates prepared by decomposition under air at 723−1123 °C for 10−12 h. Respective bands are reported at 1596, 1219, 1040, 821, 716, 711, and 689 cm^{-1} for $LaONO_3$ and 1510, 1495, 1436, 1344, 1306, 1040, 1037, 1032, 805, 754, 745, 737, and 729 cm^{-1} for anhydrous $La(NO_3)_3$.[29]

The decomposition experiments in the present study were performed under different conditions but comparable behavior appears to occur. First, the results for decomposition in Ar (sample 2, Figure 3) are discussed. Starting around 400 K, the broad OH band from 3700 to 3200 cm^{-1} and the peak at 1643 cm^{-1} found in the initial sample are lost (not shown for sample 2), and by 603 K, two single peaks at 3598 and 3507 cm^{-1} are visible. In accordance with the literature, dehydration to the anhydrous salt takes place, but isolated OH groups remain on the surface of the new compound. After completion of the thermal treatment, sample 2 still shows a OH vibration at 3594 cm^{-1} (Figure 2c) which can be assigned to a strongly bound OH group, such as that in $La(OH)_3$ after its first decomposition step to LaO(OH), at 470 K. The ongoing decomposition of this basic hydroxide leads to La_2O_3 at 573−673 K.[12] Other studies quote higher temperatures for each step of the decomposition (700 and 870 K) and remark that they depend strongly on sample preparation.[41] The XRD pattern for sample 2 further substantiates the presence of $La(OH)_3$. These hydroxyl species were already present in the initial sample or were formed from hydrated water during the initial decomposition step.

Dramatic changes in the nitrate vibrations are observed upon reaching 773 K, the temperature regime

(41) Rybakov, B. N.; Moskvicheva, A. F.; Beregovaya, G. D. *Russ. J. Inorg. Chem.* **1969**, *14*, 1531.

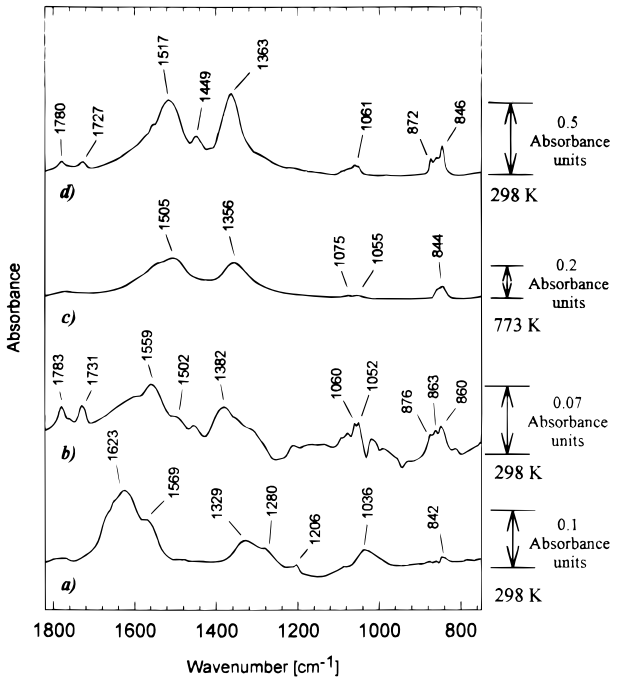

Figure 10. IR spectra of La_2O_3 (sample RP5): (a) after adsorption of CO_2 at 298 K for 30 min; (b) after a subsequent pretreatment cycle of 30 min to 773 K (spectrum taken at 298 K); (c) after adsorption of CO_2 at 773 K for 30 min; (d) after subsequent cooling to 298 K. (Each spectrum referenced to that taken just prior to CO_2 admission at 298 or 773 K, respectively.)

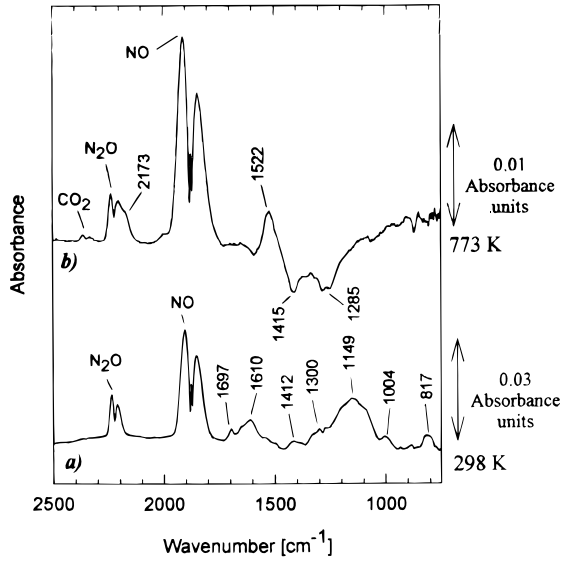

Figure 11. IR spectra of La_2O_3 (sample RP5): (a) after adsorption of NO at 298 K for 30 min and (b) after adsorption of NO at 773 K for 30 min. (Each spectrum referenced to that just prior to NO admission at 298 or 773 K, respectively.) Gas-phase peaks for NO, N_2O, and CO_2 are denoted.

for the formation of the oxynitrate, $LaONO_3$. Peaks for bidentate (1620 cm^{-1}) and unidentate (1567 cm^{-1}) nitrate groups decrease in intensity, and new species are formed (Figure 3). The peaks found at 2435, 2218, 1436, 1253, 1021, and 818 cm^{-1} are assigned to $LaONO_3$, in reasonable agreement with previous literature.[29] Further decomposition at 773 K finally leads to a completely different spectrum with peaks remaining at 2370, 1766, 1364, 1056, and 780 cm^{-1} (2390, 1770, 1370, 1061, 784 cm^{-1} at 298 K). It is obvious that nitrate and oxynitrate groups are further decomposed and only small quantities remain, as can be seen by the broadness of the 1370 cm^{-1} band and the shoulder at 1448 cm^{-1} in the spectrum at 298 K (Figure 2c). To interpret the new peaks, the following is considered. As mentioned previously, coordinated nitrate groups in the C_{2v} point group show two peaks in the 1250−1650 cm^{-1} range (NO_2 symmetric and asymmetric, υ_1 and υ_4 for unidentate). As the new spectrum reveals only one peak in this area, a surface species other than a nitrate group with this point symmetry must be present. As reported by Vratny and Honig,[42] the decomposition of rare-earth nitrates, e.g., praseodymium nitrate, can occur via a nitrite intermediate, and IR spectra of $La(NO_2)_3$ show peaks at 1408, 1365, 1325, 1250, 1175, 1030, and 845 cm^{-1}, with the peak at 1250 cm^{-1} being very intense.[31] These peak positions do not correspond with our observed results, and thus the formation of a nitrite intermediate is excluded. On the other hand, nitrate groups with D_{3h} symmetry have just one peak with doubly degenerate NO_2 stretching modes;[26] therefore, it is concluded that decomposition at 773 K finally leads to the formation of a nitrate species with D_{3h} symmetry. This implies that they are noncoordinated, or more precisely, of ionic binding character. The XRD data further indicate that a major part of the sample had already decomposed to La_2O_3. For the remaining peaks, no assignment in agreement with oxynitrate or nitrate phases reported in the literature[32] or with peaks in the initial sample is possible; consequently, it is suggested that these peaks belong to a new phase which contains ionic nitrate groups. Regarding this proposal, it is also of interest to discuss the crystallographic structure of La_2O_3. The hexagonal A-M_2O_3 sesquioxide structure of rare-earth oxides can be described as an infinite polymeric complex of OM_4 tetrahedra with shared edges, building up a tri- or bidimensional packing of layers held together by anions between the layers.[43] These O^{2-} anions can be easily exchanged by other anions, such as OH^-, CO_3^{2-}, or NO_3^-, forming so-called oxy salts, LaO_nX^{n-}. Conversely, nitrate anions can be removed from the layered structure during decomposition to form $LaONO_3$ as an intermediate. Under the given conditions, the oxynitrate further decomposes rapidly, leading to a partially collapsed layer structure with isolated, ionic nitrate groups.

Concerning decomposition under flowing oxygen (sample 1), loss of water of hydration, formation of anhydrous $La(NO_3)_3$, and further decomposition to oxynitrate as shown by the IR data (compare with Figure 1 and Table 3) are in accordance with decomposition in Ar; however, heating under O_2 does not lead to the initial formation of ionic nitrates. The spectrum taken at the end of the first thermal treatment (Figure 2a) still shows nitrate peaks at 1637, 1592, and 1351 cm^{-1} as well as oxynitrate at 2250, 1444, 1280, 1030, and 824 cm^{-1}. The second heating sequence under Ar leads to a further decrease of the initial nitrate groups and an augmentation of oxynitrate groups. Also, as observed with sample 2, the formation of ionic nitrates becomes apparent during the second treatment due to the increase around 1363 cm^{-1} and the new peaks formed at 2390, 1770, 1062, and 778 cm^{-1}, but the total amount of ionic nitrates is still small compared to

(42) Vratny, F.; Honig, J. M. *Trans. Faraday Soc.* **1960**, *56*, 1051.
(43) Caro, P. E. *J. Less-Common Met.* **1968**, *16*, 367.

sample 2. This conclusion is supported by the XRD patterns in Figure 5, which show the oxide, hydroxide, $LaONO_3$, and ionic phases in sample 1. Apparently, the presence of oxygen leads to a stabilization of the oxynitrate, which only later in the absence of oxygen further decomposes to form a phase containing ionic nitrates. The presence of $La(OH)_3$ is more pronounced in sample 2 and is associated with a peak at 3594 cm^{-1}, whereas sample 1 has peaks at 3577 and 3539 cm^{-1} which are presumably OH groups on an oxynitrate phase. The formation of the hydroxide can be again explained by the presence of gas-phase water during dehydroxylation.

NO adsorption at 298 K results in the enhancement of peaks with wavenumbers comparable to those already observed during the decomposition. The peaks at 1453, 1280, 1040, and 824 cm^{-1} can be assigned to nitrate groups in oxynitrates, those at 1385, 1063, and 779 cm^{-1} are associated with nitrate species with ionic binding character, and shoulders at 1440, 1361, and 1240 cm^{-1} can be assigned to NO_2^- groups in a nitrito or nitro configuration (see Table 4),[27, 30] but the concentration of the latter groups is low. Thus it appears that NO adsorption occurs via the formation of species already present and no new species are created. For NO adsorption at 773 K, the peak increases at 1770, 1369, 1063, and 783 cm^{-1} can clearly be assigned to nitrate groups with ionic binding character, while losses for peaks related to nitrate or oxynitrate groups (1590, 1280−1240, 1025, 826 cm^{-1}) reveal that a further decomposition of these groups occurs at this higher temperature. At 773 K other species either are unstable or adsorption sites for their formation are no longer available due to the alterations of the layer structure during heating.

To review these results, decomposition occurs via the sequential formation of anhydrous $La(NO_3)_3$, then $LaONO_3$, and finally La_2O_3. When pretreated under Ar, the oxynitrate species are transformed into a new phase consisting of ionic nitrate groups as an intermediate step in the formation of La_2O_3. During this transition, $La(OH)_3$ is also observed. Decomposition under O_2 leads partly to the oxide itself, and anhydrous nitrate and oxynitrate are formed as intermediates; however, the oxynitrate species are stable at these temperatures and are further transformed into ionic nitrates only when heated in the absence of oxygen. Adsorption of NO enhances peaks already observed during decomposition thus indicating that no new surface sites have been created and previous groups can be re-formed. The peak assignments for the species observed during decomposition are further substantiated by the experiments with NO adsorption.

4.2. Lanthanum Carbonate. Prior to discussing the experimental results for lanthanum carbonate, a summary of the literature information on this compound is presented. Various studies of the thermal decomposition behavior of $La_2(CO_3)_3$ and hydroxycarbonate have been performed,[10,44−48] and general agreement exists that both the carbonate and hydroxycarbonate decompose with $La_2O_2CO_3$ phases as intermediates. The temperature ranges given for the different decomposition steps vary due not only to the fact that the preparation of the samples again has a very important effect on the behavior of the starting material but also to the influence of experimental conditions on the process. Decomposition temperatures and kinetics differ in the presence of water or carbon dioxide.[44] The formation of hydroxycarbonate ($La_2(CO_3)_x(OH)_{2(3-x)}$) intermediates during the decomposition of $La_2(CO_3)_3$ can occur.[46] The approximate temperature ranges for the different decomposition steps are 773−973 K for the formation of $La_2O_2CO_3$ and 1073 K or above to form the oxide. This final step is reversible in CO_2-containing atmospheres.[36,48] Turcotte et al.[36] studied the crystallography of the decomposition process and found that three different polymorphic forms of $La_2O_2CO_3$ are known and can be distinguished by their IR spectrum and XRD pattern. The tetragonal I-$La_2O_2CO_3$ phase, which can be derived from the tetragonal C-form of lanthana sesquioxides, was formed first. By keeping the sample at temperatures below that required for the final oxide formation, a transformation into an intermediate monoclinic Ia-$La_2O_2CO_3$ phase occurred, and this finally transformed into hexagonal II-$La_2O_2CO_3$, whose structure is related to hexagonal A-La_2O_3.

Comparison of the spectra before (Figure 6a) and after (Figure 6b) in situ pretreatment reveals the changes in the OH vibration region. The very broad and intense band around 3600−2700 cm^{-1} belonging to hydrated, and possibly adsorbed, water is gone and separate peaks are observed at 3630, 3616, and 3484 cm^{-1} which can be assigned to hydroxyl groups in $LaCO_3OH$.[10,15,35] The OH bending mode should be visible around 1620−1650 cm^{-1}, but it is probably hidden by intense carbonate bands, thus the loss of this band cannot be observed in Figure 6b. The combination bands of the carbonate vibrations at 2899, 2525, 2347, 2186, 1824, and 1757 cm^{-1} (see Table 5) become more distinct with the removal of H_2O, and some minor peak shifts in the vibrational modes of the carbonate groups are revealed suggesting that their crystallographic surroundings had changed. The splitting of bands (into υ_1 and υ_4) as required for a C_{2v} point group is obvious in both spectra, so the carbonate groups are found to be covalently coordinated in both the initial and the pretreated materials. To determine possible changes in the crystallographic surroundings of the CO_3^{2-} groups, peaks belonging to nondegenerate vibrational modes, such as the out-of-plane bending mode (υ_6) or the C═O (υ_2) stretching vibration, are preferably used as they yield sharp peaks. Their peak position can reveal if CO_3^{2-} groups on different crystallographic sites or with different coordination are present. In spectrum 6b, υ_2 (1083 cm^{-1}) has increased in intensity and shifted 3 cm^{-1} to a higher wavenumber but, more significantly, two peaks are now found for υ_6 (844 and a shoulder at 861 cm^{-1}). Both observations suggest the formation of a different carbonate structure, in particular $La_2O_2CO_3$, and this assumption is further supported by the XRD patterns presented in Figure 7. The spectrum of the carbonate phase prior to pretreatment (Figure 7a)

(44) Petru, F.; Kutek, F.; Šatava, T. *J. Coll. Czech. Chem. Commun.* **1966**, *31*, 4459.
(45) Savin, V. D.; Mikahailova, N. P.; Eremenko, Z. V. *Russ. J. Inorg. Chem.* **1987**, *32*, 1550.
(46) Sharov, V. A.; Bezdenezhnykh, G. V. *Russ. Chem. Rev.* **1981**, *50*, 630.
(47) Akinc, M.; Sordelet, D. *Adv. Ceram. Mat.* **1987**, *2*, 232.
(48) Samuskevich, V. V.; Prodan, E. A.; Pavlyuchenko, M. M. *Russ. J. Inorg. Chem.* **1972**, *17*, 1075.

mainly reveals that it is poorly crystallized and that it contains a large amount of water due to being highly hygroscopic. For the sample after the in situ pretreatment (Figure 7b), comparison with data files[32] shows that the most intense XRD peaks can be assigned to tetragonal (I) or monoclinic (Ia) $La_2O_2CO_3$. The remaining peaks have positions comparable to those in the pattern of the initial sample, implying that the carbonate did not decompose completely during the pretreatment.

Considering the previous work just discussed, it is concluded that the pretreatment cycle utilized (30 min at 403 K, 30 min at 773 K) led to dehydration and decomposition of $La_2(CO_3)_3 \cdot 8H_2O$ to $La_2O_2CO_3$ with the polymorphic tetragonal (I) or monoclinic (Ia) forms most likely present. The hydroxyl groups cannot be removed completely, and they yield IR peaks similar to those for $LaCO_3OH$. Thus this pretreatment results in a mixed phase of partly hydrolyzed $La_2O_2CO_3$ (I, Ia) and nondecomposed $La_2(CO_3)_3$.

4.3. Lanthanum Oxide and CO_2 Adsorption on La_2O_3. The La_2O_3 oxide samples were investigated to examine the influence of purity as well as different calcination and heating pretreatments. The spectra in Figures 6c, 8a, and 6e show La_2O_3 of 99.9% (sample MC), 99.99% (sample RP1), and 99.999% (sample AL) purity levels, respectively. Peaks of hydroxyl groups and carbonate groups are observed with almost identical wavenumbers belonging to OH groups of $La(OH)_3$ and La(O)OH phases as well as unidentate carbonate. In addition, the AL sample reveals combination bands of La−O fundamental vibrational modes around 920−940 cm^{-1}. The XRD patterns for samples MC and AL are depicted in Figure 9a,b (samples MC and RP1 gave identical patterns, so the latter is not shown). The assignment of the peaks reveals that sample MC is crystallized as $La(OH)_3$, whereas for sample AL the pattern of La_2O_3 is prominent and only a small amount of $La(OH)_3$ is present. A comparison of the influence of an in situ pretreatment to 773 K (see Experimental Section) on both samples shows that the vibrations in the OH region verify that the initial MC sample consists of $La(OH)_3$ and a minor amount of La(O)OH, in agreement with the XRD pattern. Heating to 773 K does not result in complete removal of these hydroxyl groups, but rather in the transformation into La(O)OH, as shown by the peak shift from 3610 to 3585 cm^{-1}. On the other hand, the AL sample, which contains only a minor amount of $La(OH)_3$, is almost completely dehydroxylated and the few remaining OH groups exhibit a very high wavenumber of 3658 cm^{-1}, indicating isolated hydroxyl groups on the surface.[49] As for the carbonate groups, the behavior for both samples is similar: peaks around 1480 cm^{-1} are shifted to values 20−30 cm^{-1} lower. It is also possible to argue that the splitting of the υ_4 (1460−1480 cm^{-1}) and υ_1 (1366−1376 cm^{-1}) bands is reduced, which is interpreted as a diminution of covalent bonding character between the carbonate group and the metal cation.[50] Overall, these observations suggest that different types of carbonate groups are present in La_2O_3, and it is again useful to consider the polymeric layer structure found in La_2O_3 and its oxy salts. As the XRD patterns of the MC and AL samples do not show the presence of any bulk carbonate or oxycarbonate, it is assumed that the carbonate groups visible in the IR spectra are located at the surface or in the subsurface region of the layered oxide structure, which explains the differences in the peak positions due to different crystallographic surroundings.

Regarding the different purity levels in the MC, RP1, and AL samples, it is concluded that this variable is not of major importance regarding the behavior of La_2O_3. However, it is obvious that the AL sample consists mainly of La_2O_3 with minor contributions of $La(OH)_3$, which can be easily decomposed, and surface or subsurface carbonates, whereas samples MC and RP1 contain solely $La(OH)_3$. This observation is explained by the fact that the AL sample was handled under N_2, whereas the two other samples were exposed to ambient air and clearly reflect the high reactivity of La_2O_3 with atmospheric water vapor, leading to a complete transformation into the hydroxide. This important fact has to be taken into account for catalytic materials prepared from La_2O_3 stored and handled without any precautions. However, it is interesting that the samples present mainly as hydroxide exhibit a higher surface area (4.62 and 3.0 m^2/g, respectively) than La_2O_3 alone (1.14 m^2/g). This study of the influence of different calcination procedures supplies further understanding of the properties of La_2O_3. The DRIFT spectra of samples without any calcination (RP1), after calcination at 1023 K in air (RP2), after calcination at 1023 K in O_2 (RP3), and after 1273 K in O_2 (RP5) are compared in Figure 8. Calcination in oxygen at 1023 K (RP3, Figure 8c) results in a spectrum similar to that of the initial sample (RP1, Figure 8a), i.e., unidentate carbonate groups are present as well as hydroxyl groups belonging to $La(OH)_3$ and La(O)OH. The latter are less intense on the calcined sample, as expected, and examination of the XRD patterns (Figure 9a, which is identical with sample RP1, and Figure 9d) also shows that the calcined sample is a mixture of La_2O_3 and $La(OH)_3$, whereas the uncalcined sample consists only of the hydroxide. It is pointed out that the calcined sample was exposed to air during the XRD runs, thus the calcination probably resulted in dehydroxylation and formation of solely La_2O_3, as the hydroxide is not stable at 1023 K,[12,13] but the $La(OH)_3$ phase was easily restored due to the facile reaction of La_2O_3 with atmospheric water vapor. Consistent with this, sample RP5, which was stored and handled under N_2, showed no indication of bulk $La(OH)_3$ in the XRD pattern (Figure 9e) and only a trace of isolated OH groups in the DRIFT spectrum (Figure 8d), whereas La−O combination vibrations are clearly resolved. Hence, the high-temperature calcination at 1273 K results in complete dehydroxylation to La_2O_3, and it also reduces the concentration of carbonate groups in comparison to sample RP3, which was treated at 1073 K. Unidentate and bidentate carbonate groups are now present, suggesting that changes occurred in the polymeric layer structure which now allow different coordination of carbonate groups at the surface or in the subsurface region. Finally, calcination in air leads to an interesting alteration of the La_2O_3 sample. Hydroxyl groups of $La(OH)_3$ and La(O)OH due to rehydroxylation are again visible in the DRIFT spectrum, and the

(49) Griffiths, D. M.; Rochester, C. H. *J. Chem. Soc. Faraday Trans. 1* **1977**, *73*, 1510.

(50) Hair, M. L. *Infrared Spectroscopy in Surface Chemistry*; Marcel Dekker: New York, 1967.

respective XRD patterns for these phases are also observed (Figures 8b and 9c),[6,51] but in contrast to all the other samples, pronounced carbonate groups with well-resolved bands are found. They are assigned to the hexagonal II-$La_2O_2CO_3$ phase, which is substantiated by the XRD pattern consisting mainly of oxycarbonate peaks in hexagonal modification, with some minor contributions from monoclinic Ia-$La_2O_2CO_3$, La_2O_3 itself, and the two previously mentioned hydroxide phases. The result is understandable considering that the dry air (grade 1) used for the calcination can contain up to 500 ppm CO_2, and treatment at 1023 K allows a thorough reaction between CO_2 and oxygen anions to form bulk oxycarbonate in the crystallographic structure stable at this temperature.[36] It is again noted that the samples consisting mainly of La_2O_3 (RP4 or RP5) have extremely low surface areas of 0.71 and 0.87 m^2/g, respectively, which is due to sintering at the higher calcination temperatures. In contrast, the samples subjected to lower treatment temperatures have higher surface areas of 3.9 and 4.7 m^2/g and are composed of $La(OH)_3$ and La_2O_3 (RP3) or oxycarbonate and hydroxide phases (RP2).

CO_2 adsorption was conducted to probe the Lewis basicity of O^{2-} anions on the surface and to compare carbonate peak positions with the groups found in the original samples. A sample (RP5) with a low concentration of surface or subsurface carbonate groups was chosen to guarantee a considerable interaction of CO_2 with the oxide surface. Adsorption of CO_2 at 298 K leads to the initial formation of bidentate carbonates which convert into unidentate species during heating to 773 K, whereas adsorption at 773 K immediately produces unidentate groups (Figure 10). The final spectra taken at 298 K (Figure 10b,d) reveal similar peak positions but varying intensities. In comparison to the carbonate groups already present in the different oxide samples, higher wavenumbers for the ν_4 vibrations and an augmented splitting between ν_4 and ν_1 is observed (compare Table 5). As the $\Delta\nu$ value for the peak splitting correlates inversely with the strength of the Lewis basic sites,[20,21] the observation of a relatively high splitting suggests only medium Lewis basicity for the O^{2-} anions involved. Because of the experimental conditions chosen, the carbonate groups formed should be located at the surface of the sample. As a second method to investigate the basicity of La_2O_3, NO adsorption was performed at 298 and 773 K (Figure 11 and Table 6). At both temperatures, the interaction of NO with sample RP5 leads only to relatively weak peaks, but they still allow one to distinguish among different adsorbed species. At 298 K, bidentate and bridged nitrate groups (NO_3^-), nitro groups (NO_2^-) and a broad signal tentatively assigned to NO^- and its dimer $N_2O_2^{2-}$ are found.[52] In contrast, the spectrum taken at 773 K shows only a peak for unidentate nitrate groups, while other peaks are most likely obstructed by the loss of peak intensity for carbonate groups, which occurs together with the detection of gas-phase CO_2. This interesting observation is interpreted as the key to understanding the interaction of NO with the surface. It is proposed that the presence of NO leads to the decomposition of carbonate groups, thus freeing O^{2-} anions and allowing the formation of nitrite and nitrate groups. Hence, the process can be viewed as an exchange reaction taking place with the O^{2-} anions functioning as adsorption centers. The total reaction can be understood as NO disproportionation to nitrate or nitrite plus nitrogen, which has been observed as a reaction product.[1] Adsorbed NO^- (and the dimer) are presumed to be possible intermediates of the disproportionation reaction,[52] and the following equations represent the surface chemistry taking place:

$$6NO + 2CO_3^{2-} \rightarrow 2CO_2 + 4NO_2^- + N_2 \quad (1)$$

$$10NO + 2CO_3^{2-} \rightarrow 2CO_2 + 4NO_3^- + N_2 \quad (2)$$

Thus, the adsorption experiments with NO reveal the interesting surface chemistry that appears to take place on La_2O_3 containing residual carbonate groups, which might be rooted in the unique layer structure of the material. It is possible that these types of exchange reactions might play a role in catalytic reactions on La_2O_3 such as NO decomposition.[1,52]

5. Summary

The work presented here provides a comprehensive FTIR and XRD data set for the characterization of La_2O_3, $La(CO_3)_3$, and $La(NO)_3$, the thermal behavior of these compounds in the presence and absence of O_2, the adsorption of NO on decomposed $La(NO_3)_3$, and CO_2 and NO adsorption on La_2O_3. The compounds present were determined together with the sample surface area, another parameter important for catalytic applications. Thermal treatment of $La(NO_3)_3$ up to 773 K leads to decomposition, and the intermediates formed depend on the gas phase present. It was found that decomposition under flowing O_2 is less complete and stops with the formation of a stable oxynitrate phase, $LaONO_3$, in addition to La_2O_3. For decomposition in Ar, the oxynitrates were only an intermediate during the further transformation to La_2O_3 and a nitrate phase with an ionic (noncoordinated) character, i.e., no direct coordination with specific La cations. Taking the polymeric layer structure of La_2O_3 and its oxy salts into account, it appears that the oxynitrate is stabilized in the presence of O_2, whereas the layers partially collapse during further decomposition in Ar to form the ionic nitrate phase. NO adsorption at 298 K on the decomposed sample resulted in the formation of oxynitrates, nitrite groups, and ionic nitrates, whereas only the ionic nitrate groups were produced after adsorption at 773 K. Therefore, adsorption of NO leads not to the formation of the type of nitrate groups initially found in the sample but to more stable species which remain after the decomposition sequence, presumably at the surface. Thus, the thermal treatment used for the decomposition procedure results in irreversible structural changes, such as a partial collapse of the polymeric layers, which determines the properties of the sites capable of NO adsorption. Consequently, the use of $La(NO_3)$ as an oxide precursor, e.g., for supported La_2O_3 catalysts, will require carefully chosen decomposition conditions because the actual decomposition is complicated and can lead to different phases containing nitrate groups depending on the temperature and the gaseous medium.

Application of the same thermal treatment to $La_2(CO_3)_3 \cdot 8H_2O$ led to a partial transformation into La_2O_2-

(51) Shafer, M. W.; Roy, R. *J. Am. Ceram. Soc.* **1959**, *42*, 563.
(52) Klingenberg, B.; Vannice, M. A., to be published.

CO_3, which was present mainly in its tetragonal (I) and monoclinic (Ia) forms. This result shows that the decomposition of $La_2(CO_3)_3$ to yield La_2O_3 requires very high temperatures and will give low surface areas.

Three commercially available La_2O_3 samples with different purity levels were investigated. The handling of the material, rather than the purity, is the dominant factor in determining their behavior. Samples stored and handled in ambient air are present as the hydroxide, which can be transformed into the oxide by heating to at least 773 K under either Ar or oxygen; however, the samples rapidly rehydroxylate when contacted with ambient air. Only storage under an inert gas such as N_2 guarantees the absence of hydroxide formation. Carbonate groups, formed readily from CO_2 in the surrounding air, are always present and cannot be removed completely by heating to 773 K, and they appear to be located at the surface or in the subsurface region of the layered oxide structure. One sample as received was subjected to varying initial calcination steps which differed in the temperature range and the gaseous medium used. Thermal treatment in O_2 at 1023 K led to a sample with some surface and subsurface carbonates left. Hydroxyl groups were removed at that temperature as found when the sample was not air exposed and stored under N_2; however, they are easily re-formed when the sample is contacted with ambient air. Thermal treatment in dry air at 1023 K led to an oxide containing a considerable amount of bulk hydroxy- and carbonate phases, with the latter being mainly hexagonal II-$La_2O_2CO_3$. These results imply that the initial calcination procedure can determine the final composition of the sample. High temperatures and a CO_2-free atmosphere are needed to yield a pure oxide sample; however, such a procedure produces considerable sintering of the sample and a major loss of surface area. If samples with higher surface areas are required, i.e., lower temperatures are used, the presence of significant amounts of OH and carbonate groups cannot be avoided.

The Lewis basicity of O^{2-} anions in La_2O_3 was indicated by CO_2 adsorption to be of medium strength. The carbonate groups formed are mainly unidentate and are located at the surface and in the subsurface region of the sample. NO adsorption revealed interesting surface chemistry, i.e., nitrate and nitrite groups replace carbonate groups via a disproportionation reaction which also gives N_2, and NO^- and its dimer species on the surface were also identified. Gas-phase CO_2 is also produced. This reaction may be important in the catalytic sequence of NO decomposition and is possibly also of interest for other catalytic processes on La_2O_3 involving NO_x.

Finally, this study provides a comprehensive background for the preparation of La_2O_3 catalysts. It shows that the preparation and handling procedures determine the composition, chemical state, and surface area of the sample, and a compromise between the presence of hydroxide and carbonate groups on one hand and a relatively high surface area may have to be made. Interesting surface chemistry following NO adsorption has been observed which involves carbonate groups. Consequently, it will be important to determine which states of the material are present and actually beneficial under reaction conditions. This approach is being used in further studies of catalytic reactions on La_2O_3 involving NO, the effect of Sr promoters, and the preparation of La_2O_3 catalysts by dispersing a precursor La compound on Al_2O_3 or SiO_2.

Acknowledgment. The authors thank the NSF for an equipment grant to acquire the DRIFTS system (CTS-9311087), the German Alexander-von Humboldt Foundation for the award of a research fellowship for B.K., and Mobil Corp. for partial support of this study.

CM9602555